Raman effect in AlGaAs waveguides for subpicosecond pulses

Y.-H. Kao[a] and M. N. Islam
The University of Michigan, Ann Arbor, Michigan 48109

J. M. Saylor, R. E. Slusher, and W. S. Hobson
AT&T Bell Laboratories, Murray Hill, New Jersey 07974

The Raman effect in semiconductor waveguides below half-gap is studied both experimentally and numerically. We report the depolarized Raman gain spectra up to 300 cm^{-1} in Al$_{0.24}$Ga$_{0.76}$As at pump wavelengths of 0.515 and 1.55 μm from the measurement of the absolute Raman scattering cross sections using GaAs as a reference scatterer. In addition, the coupled propagation equations for the AlGaAs waveguides are modified to include the Raman effect. By solving the coupled propagation equations numerically, we verify that the energy transfer between two orthogonally polarized pulses demonstrated in previous pump-probe experiments [M. N. Islam *et al.*, J. Appl. Phys. **71**, 1927 (1992)] is caused by Raman effect. We also show numerically that the Raman effect induces spectral distortions on the pulses, and the energy transfer is inversely proportional to the pulse widths. The energy transfer results in a severe cross-talk problem for sub-picosecond pulses in AlGaAs waveguides. For example, the energy exchange is about 30% for 300 fs pulses under π phase shift conditions. Therefore, the Raman effect limits the performance of semiconductor waveguides in optical switching applications for sub-picosecond pulses. © *1995 American Institute of Physics.*

I. INTRODUCTION

Semiconductor waveguides operating below half-gap have been of interest for making compact, integrated optical switching devices because of their high nonlinear refractive index and negligible nonlinear two-photon absorption. Among the various semiconductor materials, the GaAs/AlGaAs material system is very attractive because a mature fabrication technology already exists. Also, the half-bandgap energy of this material can cover the infrared window between 1.3 and 1.6 μm, which is important for optical communications. The nonlinear properties of GaAs/AlGaAs, such as nonlinear refractive index and two photon absorption, have been extensively studied.[1-3] All-optical switching devices in AlGaAs waveguides, such as Mach-Zehnder interferometers[4] and nonlinear directional couplers,[5] that operate below mid-gap have also been demonstrated. Although some authors have pointed out that three-photon absorption is a limitation to the attractiveness of AlGaAs waveguides,[6] this factor can be avoided by reducing the intensity and increasing the device length. On the other hand, we believe that the Raman effect, which is proportional to imaginary part of $\chi^{(3)}$ and previously unconsidered, provides a limitation of semiconductor waveguides operated at short pulse widths for nonlinear index applications.

In this paper we study the Raman effect in AlGaAs waveguides. We begin in Sec. II by measuring the spontaneous Raman scattering cross sections at 0.515 μm with GaAs as a reference scatterer. The Raman gain spectra are calculated from the scattering cross sections in the spectral range from 0 to 300 cm^{-1} at pump wavelengths of 0.515 and 1.55 μm. Below 80 cm^{-1}, the Raman gain appears to be linearly dependent on frequency. In Sec. III we model the energy

interaction between pump and probe pulses by modifying the coupled propagation equations for AlGaAs waveguides with the inclusion of the Raman effect. The coefficients of the Raman terms are related to the Raman gain. In Sec. IV the coupled propagation equations are solved numerically by substituting the measured Raman gain and the experimental parameters. We verify that the energy exchange between the orthogonally polarized pump and probe pulses in the previous experiment[1] is caused by the Raman effect. Furthermore, the Raman effect induces a spectral distortion for pulses propagating in semiconductor waveguides, which is different from the soliton self-frequency shift found in optical fibers.[7] Finally, we find that the amount of energy exchange (crosstalk) due to the Raman effect is inversely proportional to the pulse widths, which can degrade the switching performance of semiconductor waveguides using subpicosecond pulses.

II. RAMAN GAIN SPECTRA OF Al$_{0.24}$Ga$_{0.76}$As

We obtain the Raman gain spectra of Al$_{0.24}$Ga$_{0.76}$As from the experimentally measured spontaneous Raman scattering cross sections. We determine the absolute Raman scattering cross section in Al$_{0.24}$Ga$_{0.76}$As using a comparison technique in which the cross section is measured relative to a GaAs scatterer. Because the spectral width of optical pulses used in optical switching applications is narrow ($\sim$50 cm^{-1} for a 300-fs Gaussian pulse) compared to the Raman gain spectrum for AlGaAs material, the pulses can only excite the Raman gain at low frequencies. Therefore, we focus on the measurement of the low frequency Raman scattering cross section.

The experimental setup for measuring the Raman scattering cross sections of Al$_{0.24}$Ga$_{0.76}$As is illustrated schematically in Fig. 1. The experiments are performed in the back-

[a]Electronic mail: ykao@engin.umich.edu

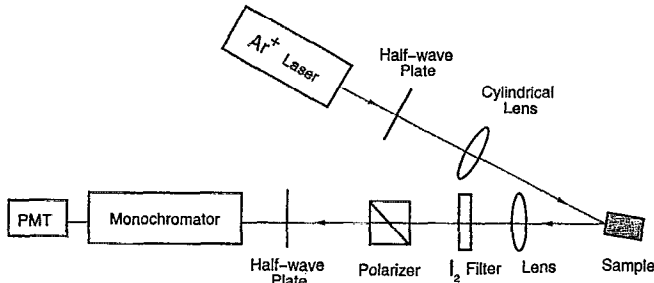FIG. 1. Experimental setup of Raman scattering measurement (PMT = photomultiplier tube).
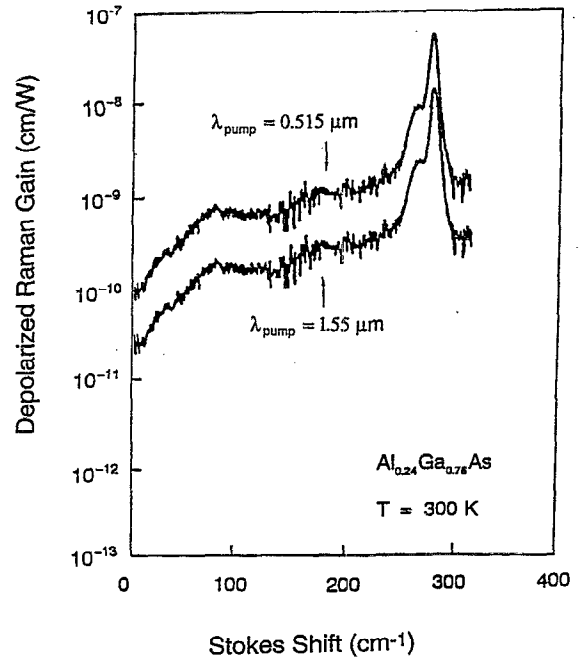

FIG. 2. Depolarized Raman gain spectra for $Al_{0.24}Ga_{0.76}As$ at pump wavelengths of 0.515 μm (upper curve) and 1.55 μm (lower curve) at room temperature.

scattering configuration at room temperature. The pump source is a single spatial mode cw argon ion laser at a wavelength of 0.515 μm, which is focussed to a line 50 μm by 0.2 cm. The half-wave plate in front of the sample is used to rotate the pump polarization, and an I_2 absorption cell filter is used to attenuate the Rayleigh scattered light from the pump laser. The Raman scattered light is focussed onto a SPEX scanning double monochromator and detected by a cooled Hamamatsu R585 photomultiplier tube (PMT) with a dark count of approximate 3 counts/sec. Finally, we use a polarizer to select the polarization of the Raman scattered light and a half-wave plate to rotate this polarization to horizontal for analysis by the monochromator.

The GaAs and $Al_{0.24}Ga_{0.76}As$ samples are grown by organometallic vapor phase epitaxy. To reduce oxidation, the samples are capped with 200 Å GaAs, which is stripped by reactive ion etching just before measurements, and are kept in helium gas. The oxidation can cause surface roughening and disorder-induced scattering. The samples are mounted adjacent to each other on a translational stage in order to keep constant collection geometry while sliding in and out of the sampling volume. The sample holder is placed inside a helium gas cell during the experiments to prevent the low frequency Raman scattering by air.

We measure the scattered light from the [100] surface of each sample for the four different configurations listed in Table I.[10,11] The Raman scattering cross sections are written in terms of the irreducible second rank Raman tensor components a, b, and d. After calibration of the Raman scattering cross sections according to the differences in scattering

length, reflection losses, and solid angles due to the different indices of refraction between GaAs and $Al_{0.24}Ga_{0.76}As$,[10] we obtain the relative Raman cross section of $Al_{0.24}Ga_{0.76}As$, with respect to GaAs. From the absolute Raman cross section of GaAs measured in Refs. 8 and 9, we then obtain the absolute Raman cross sections of $Al_{0.24}Ga_{0.76}As$ for four configurations in Table I. From those Raman cross sections, we extract the three irreducible components a, b, and d and then calculate the three nonzero fourth rank Raman tensors I_{1111}, I_{1212}, and I_{1122} (see Table I) for $Al_{0.24}Ga_{0.76}As$. Finally, we obtain the Raman gain (g_{ijkl}^{Ram}) from the Raman scattering cross section (σ_{ijkl}), which is proportional to the fourth rank Raman tensor I_{ijkl},[11] using the relation[12]

$$g_{ijkl}^{Ram}(cm/W) = \frac{\sigma_{ijkl}(1/cm \cdot sr \cdot cm^{-1})\lambda_s^3}{c^2 h \epsilon (n_0 + 1)}, \quad (2.1)$$

where σ_{ijkl} is the Raman cross section, λ_s is the wavelength of the scattered light, ϵ is the dielectric constant at the scattered light wavelength, h is Planck's constant, and n_0 is the Bose-Einstein factor.

In Fig. 2 we present the depolarized Raman gain spectra ($g_{1212}^{Ram}(\omega)$) for $Al_{0.24}Ga_{0.76}As$ at pump wavelengths of 0.515 and 1.55 μm. The Raman gain spectrum at 1.55 μm is obtained by scaling from the spectrum at 0.515 μm. This is because when the pump wavelength is away from the Raman resonances, the Raman scattering cross section is inversely proportional to the pump wavelength. This inverse relationship is due to the fact that photomultiplier tube measures photon number instead of photon energy. The depolarized Raman gain at 100 cm^{-1} is about 10^{-10} cm/W, which is two orders of magnitude larger than that in silica fibers.[13] We find that the Raman gain below 80 cm^{-1} appears to be linearly

TABLE I. Selection rules for Raman scattering from surface [100] for the zinc-blende structure, where a, b, and d are the irreducible components of the second rank Raman tensors. The nonzero fourth rank Raman tensors are $I_{1111}=a^2+4b^2$, $I_{1122}=(a^2-2b^2+d^2)/2$, and $I_{1212}=d^2$.

Configuration	Incident polarization	Scattered polarization	Raman intensity
1	[01$\bar{1}$]	[01$\bar{1}$]	$a^2+b^2+d^2$ (LO)[a]
2	[011]	[01$\bar{1}$]	$3b^2$
3	[010]	[001]	d^2(LO)[a]
4	[010]	[010]	a^2+4b^2

[a]Longitudinal optical phonons.

J. Appl. Phys., Vol. 78, No. 4, 15 August 1995

Kao *et al.* 2199

dependent on frequency, and the slopes (s_1, s_2, and s_3) of the Raman gain spectra (g_{1111}^{Ram}, g_{1122}^{Ram}, and g_{1212}^{Ram}) below 80 cm^{-1} follow the relations

$$s_1 \simeq 2s_3 \quad \text{and} \quad s_2 \simeq 0.5s_3, \tag{2.2}$$

where $s_3 \simeq 3.28 \times 10^{-12}$ cm/W/cm^{-1} at a 1.55 μm pump wavelength. We will show in the next two sections that the slopes of the Raman gain spectra dominate the Raman effect for sub-picosecond pulses.

III. COUPLED PROPAGATION EQUATIONS FOR AlGaAs WAVEGUIDES

Raman scattering in semiconductors arises from the interaction of light with optical phonons. Following the density matrix formalism[14] and treating the material as a three level system, we derive the nonlinear polarization $\mathbf{P}_{Raman}^{(3)}(z,t)$, which is responsible for the Raman process. In particular,

$$P_i^{(3)}(z,t) = E_j(z,t) \int_0^t \chi_{ijkl}^{(3)}(t-t', t-t'; 0)$$

$$\times \{ E_k^*(z,t') E_l(z,t') + E_k(z,t') E_l^*(z,t') \} dt', \tag{3.1}$$

where $P_i^{(3)}(z,t)$ is the ith vector component of $\mathbf{P}_{Raman}^{(3)}(z,t)$, $E_j(z,t)$ is the jth vector component of the electric field and $\chi_{ijkl}^{(3)}(t-t', t-t'; 0)$ is the third order susceptibility, which will be abbreviated as $\chi_{ijkl}^{(3)}$. For a system with cubic symmetry like AlGaAs, the third order susceptibility can be expressed as

$$\chi_{ijkl}^{(3)} = \chi_{1122}^{(3)} \delta_{ij} \delta_{kl} + \chi_{1221}^{(3)} \delta_{il} \delta_{jk} + \chi_{1212}^{(3)} \delta_{ik} \delta_{jl}$$

$$+ (\chi_{1111}^{(3)} - \chi_{1122}^{(3)} - \chi_{1221}^{(3)} - \chi_{1212}^{(3)}) \delta_{ijkl}. \tag{3.2}$$

Thus, Eq. (3.1) becomes

$$P_i^{(3)} = 2E_i(z,t) \int_0^t \chi_{1122}^{(3)} \mathbf{E}^*(z,t') \cdot \vec{E}(z,t') dt' + \mathbf{E}(z,t)$$

$$\cdot \int_0^t \mathbf{E}^*(z,t')(\chi_{1221}^{(3)} + \chi_{1212}^{(3)}) E_i(z,t') dt' + \mathbf{E}(z,t)$$

$$\cdot \int_0^t \mathbf{E}(z,t')(\chi_{1221}^{(3)} + \chi_{1212}^{(3)}) E_i^*(z,t') dt' + 2E_i(z,t)$$

$$\times \int_0^t (\chi_{1111}^{(3)} - \chi_{1122}^{(3)} - \chi_{1221}^{(3)} - \chi_{1212}^{(3)})$$

$$\times E_i^*(z,t') E_i(z,t') dt'. \tag{3.3}$$

To derive the coupled propagation equations for two orthogonally polarized pulses, we express the total electric field and the nonlinear polarization in the waveguide as

$$\mathbf{E}(z,t) = [U(z,t) e^{ik_0 z} \hat{e}_x + V(z,t) e^{il_0 z} \hat{e}_y] e^{-i\omega_0 t} + c.c.,$$

$$\mathbf{P}_{Raman}^{(3)}(z,t) = [\phi(z,t) e^{ik_0 z} \hat{e}_x + \psi(z,t) e^{il_0 z} \hat{e}_y] e^{-i\omega_0 t} + c.c. \tag{3.4}$$

Substituting Eq. (3.4) in Eq. (3.3) and using the result in the evolution equation,[15,16] we obtain

$$i \frac{\partial U}{\partial z}\bigg|_{Raman} = -\frac{4\pi\omega_0^2}{c^2 k_0} \left\{ U(z,t) \int_0^t \chi_{1111}^{(3)} |U(z,t')|^2 dt' \right.$$

$$+ U(z,t) \int_0^t \chi_{1122}^{(3)} |V(z,t')|^2 dt' + V(z,t)$$

$$\times \int_0^t \chi_{1212}^{(3)} V^*(z,t') U(z,t') dt' + V(z,t)$$

$$\left. \times \int_0^t \chi_{1212}^{(3)} V(z,t') U^*(z,t') e^{2i(l_0-k_0)z} dt' \right\}, \tag{3.5}$$

and a similar result for $i\partial V/\partial z|_{Raman}$, where we have used the intrinsic symmetry relation $\chi_{1221}^{(3)} = \chi_{1212}^{(3)}$. The fourth term in Eq. (3.5) can be neglected for AlGaAs waveguides because of the large phase factor $[(l_0-k_0) \simeq 20 \gg 1]^1$. The nonlinear gain G for a beam propagating in a waveguide is usually defined as

$$\frac{\partial U}{\partial z} = G \cdot I \cdot U, \tag{3.6}$$

where U is the field of the beam and I is the beam intensity. Therefore, we can relate the imaginary part of $\chi_{ijkl}^{(3)}$, $Im(\chi_{ijkl}^{(3)})$, to the Raman gain coefficient, g_{ijkl}^{Ram}, as

$$\frac{4\pi\omega_0^2}{c^2 k_0} Im[\chi_{ijkl}^{(3)}(t-t', t-t'; 0)]$$

$$= -\int_{-\infty}^{\infty} \frac{g_{ijkl}^{Ram}(\omega)}{2A_{eff}} e^{-i\omega(t-t')} d\omega, \tag{3.7}$$

where A_{eff} is the effective area of waveguides.

Since the spectral width of our pulse is small compared to the Raman gain spectrum, we expand $g_{ijkl}^{Ram}(\omega)$ as a Taylor series in the frequency domain and retain only the first two terms. The first term is ignored because it is independent of frequency and it only changes the Kerr coefficients slightly.[15] Then, we obtain the coupled propagation equations for two orthogonally polarized pulses, including the Raman terms, in AlGaAs waveguides

$$\frac{\partial U}{\partial z} = \frac{i2\pi n_2 U}{\lambda A_{eff}} (|U|^2 + \tfrac{2}{3}|V|^2) - \frac{\alpha}{2} U - \frac{U}{2A_{eff}} \{\beta_{1111}|U|^2$$

$$+ \beta_{1122}|V|^2 + \beta_{1212}(UV^* + U^*V)\}$$

$$- \frac{iU}{4\pi A_{eff}} \left(s_1 \frac{\partial}{\partial t}|U|^2 + s_2 \frac{\partial}{\partial t}|V|^2 \right)$$

$$- \frac{i}{4\pi A_{eff}} s_3 V \frac{\partial}{\partial t} UV^*, \tag{3.8}$$

and a similar result for $\partial V/\partial z$, where n_2 is the nonlinear refractive index, α is the linear absorption coefficient, β_{ijkl}'s are the anisotropic two photon absorption coefficients,[17] and s_i's are the slopes of Raman gain spectra at low frequencies. For numerical simplicity, we ignore the linear absorption term and normalize Eq. (3.8) as
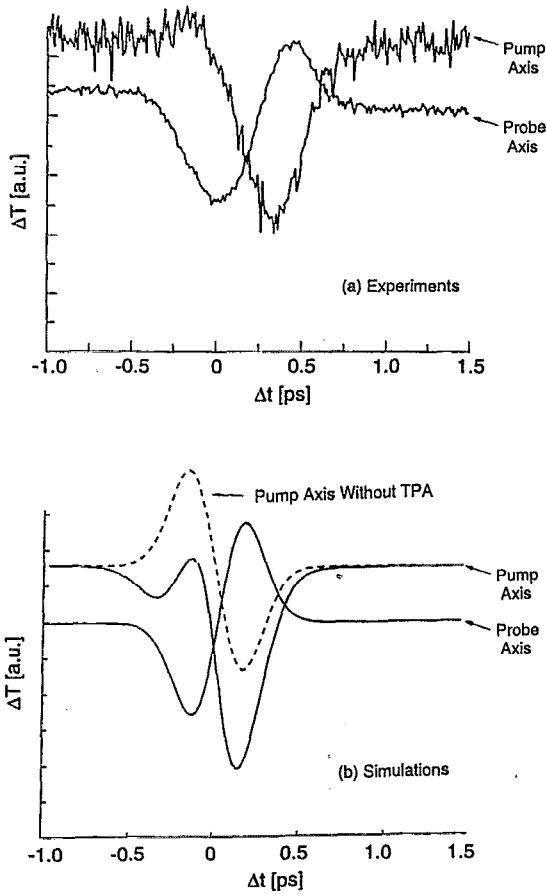
Kao *et al.*

FIG. 3. (a) Time-resolved pump-probe data for a $Al_{0.2}Ga_{0.8}As$ bulk waveguide using 285-fs pulses at 1.67 μm with polarizer at output along pump axis and probe axis. The pump is orthogonally polarized to the probe. (b) Numerical result for two orthogonally polarized pulses propagating through a $Al_{0.2}Ga_{0.8}As$ waveguide under the same conditions as (a). The dashed curve shows the differential transmission of the pump pulse without the TPA effect.

$$\frac{\partial U}{\partial z} = i|U|^2 U + i\,\frac{2}{3}\,|V|^2 U - \frac{\lambda U}{4\pi n_2}\,\{\beta_{1111}|U|^2 + \beta_{1122}|V|^2$$

$$+ \beta_{1212}(UV^* + U^*V)\} - ic_1 U\,\frac{\partial}{\partial t'}|U|^2$$

$$- ic_2 U\,\frac{\partial}{\partial t'}|V|^2 - ic_3 V\,\frac{\partial}{\partial t'}\,UV^*, \qquad (3.9)$$

where $t' = t/t_c$ $(t_c = \tau/1.177$ for Gaussian pulse with pulse width τ), and

$$c_i = \frac{\lambda s_i}{8\pi^2 n_2 t_c}, \qquad (3.10)$$

which is similiar to the expression of soliton self frequency shift coefficient.[7] The first five terms on the right hand side of Eq. (3.9) contribute to self-phase modulation (SPM), cross-phase modulation (XPM), anisotropic two photon absorption (TPA), frequency distortion from the self-Raman gain g_{1111}^{Ram}, and frequency distortion from the g_{1122}^{Ram}. The last

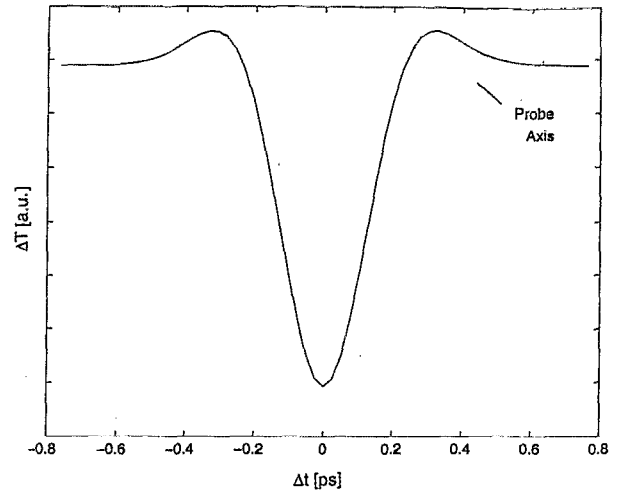FIG. 4. Differential transmissions of the probe out of a $Al_{0.2}Ga_{0.8}As$ waveguide as a function of time separation (Δt) in the absence of SPM and XPM.

term is related to the depolarized Raman gain g_{1212}^{Ram}, which produces both energy transfer between two pulses and frequency distortion.

IV. SIMULATION RESULTS AND DISCUSSION

The simulation results of this paper confirm that the energy transfer observed in the pump-probe measurements[1] earlier is induced resulting from the Raman effect mechanism. For example, Fig. 3(a) shows the pump-probe measurement results previously reported.[1] These results were measured in a 7.2 mm long $Al_{0.2}Ga_{0.8}As$ bulk waveguide. The pump and probe were orthogonally polarized 285-fs pulses at a wavelength of 1.67 μm. The pump intensity was 3.85 GW/cm^2, which produced a π phase shift, and the probe intensity was about 1% of the pump. The differential transmissions (ΔT) as a function of time separation (Δt) were measured by putting a polarizer along the pump and probe polarization axes. A transfer of energy between the two axes was observed. The probe gave energy to the pump when $\Delta t < 0$, and the probe gained energy from the pump when $\Delta t > 0$.

Applying the same conditions as the pump-probe experiment to Eq. (3.9) and assuming Gaussian pulses for the pump and the probe, we obtain the results shown in Fig. 3(b). We use $n_2 = 1.8 \times 10^{-14}$ cm^2/W, $\beta_{1111} = 0.26 \times 10^{-4}$ cm/MW,[1] $\beta_{1122} = 0.59\beta_{1111}$, and $\beta_{1212} = 0.58\beta_{1111}$.[17] The coefficients c_i ($c_1 = 0.12$, $c_2 = 0.03$, and $c_3 = 0.06$) are calculated by substituting the slopes of Raman gain spectra to Eq. (3.10). The curves shown in Fig. 3 are drawn in arbitrary units and displaced to highlight the transmission change for each pulse. The simulated peak-to-peak transmission change of the probe pulse is about 35%, which agrees with the value of 30% obtained from the previous experimental result.[1] The agreement between the experiment and simulation verifies that the low frequency depolarized Raman gain of the AlGaAs waveguide is responsible for the energy exchange between two orthogonally polarized pulses.
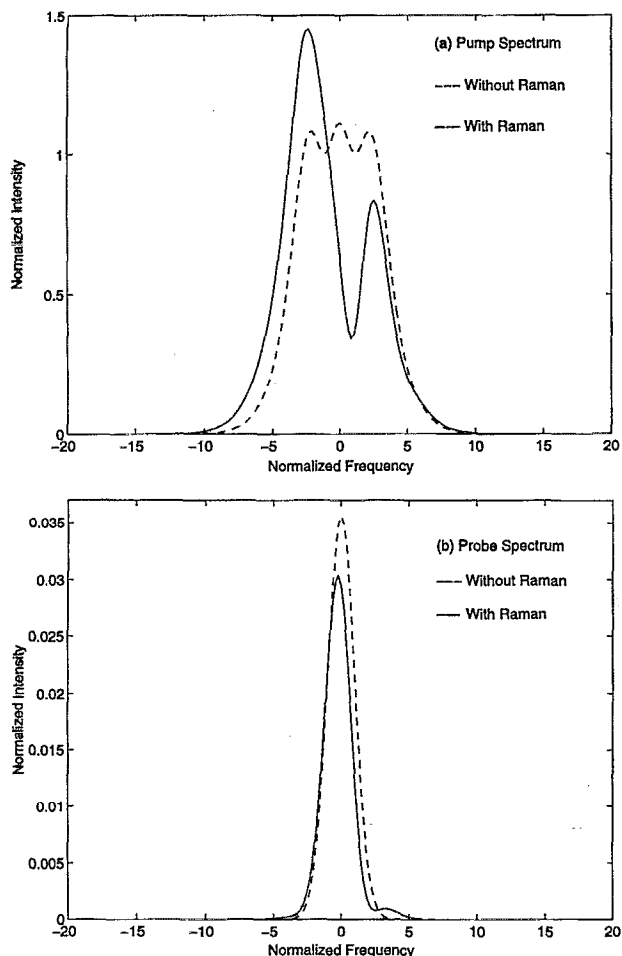
FIG. 5. Frequency spectra for the pump pulse (a), and for the probe pulse (b) when $\Delta t = -0.13$ ps. The dashed curves show the pulse spectra without the Raman effect, and the solid curves show the spectra with the Raman effect.
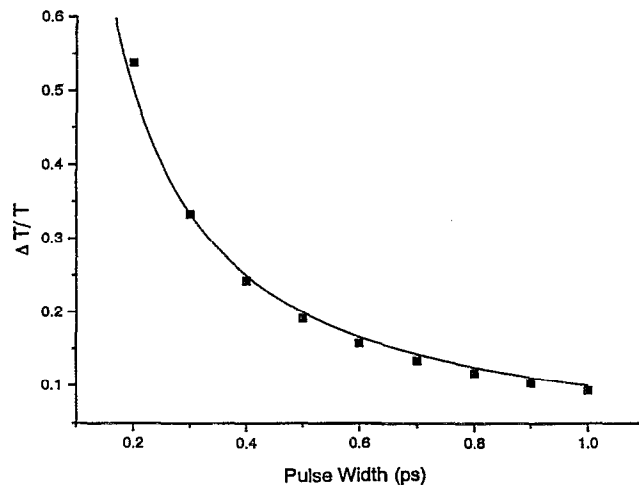

FIG. 6. The normalized peak-to-peak differential transmission of the probe as a function of pulse width. The dots are the results from simulation. The solid curve is inversely proportional to the pulse width.

This model enables us to obtain greater insight into the results of Fig. 3. First, the sign of the energy transfer (ΔT) depends on the sign of the time separation (Δt) between the pump and the probe. This is due to the self-phase modulation (SPM) on the pump pulse. When $\Delta t < 0$, the probe overlaps with the leading edge of the pump, which is red-shifted by the SPM. The pump gains energy from the probe because the lower frequencies of the pump extract energy from the higher frequencies of the probe due to the depolarized Raman effect.[14] To confirm this argument we deliberately drop the SPM term in Eq. (3.9) and show the differential transmission of the probe in Fig. 4. In this case, the probe always transfers energy to the pump, because the self-Raman effect leads to amplification of the lower frequencies of the pump at the expense of its higher frequencies [see Fig. 5(a)]. When the probe overlaps with the pump pulse, the depolarized Raman effect causes energy transfer from the higher frequencies of the probe to the lower frequencies of the pump. In addition, since SPM broadens the pulse spectrum and therefore the pulse excites wider Raman gain spectrum, SPM enhances the energy exchange. For example, the simulated energy transfer is 35% of the probe between 285 fs pulses with

SPM, and it is only 9% without SPM. We also verify that the energy exchange between the pump and the probe due to the Raman effect is conserved (i.e., the energy leaving one pulse results in the other). This conservation result is masked in Fig. 3 because the pump pulse suffers stronger TPA than the probe. On the other hand, the dashed curve in Fig. 3(b) shows the differential transmission of the pump without TPA, thus demonstrating that the energy transfer is conserved and caused by the Raman effect.

Futhermore, because of the frequency dependent Raman gain, the Raman effect induces the spectral distortion and asymmetry shown in Fig. 5. The time separation between two pulses is chosen at about -0.1 ps when the probe transfers maximum energy to the pump. The dashed curves represent spectra broadened by SPM under π phase shift conditions; the solid curves represent the spectra distorted by the Raman effect and SPM under the same conditions. The spectral distortion of the pump pulse [Fig. 5(a)] is mainly caused by the self Raman effect, which transfers energy from the high frequencies to the lower frequencies. On the other hand, the probe spectrum is distorted by the depolarized Raman gain because the energy transfers from the higher frequencies of the probe to the pump pulse.

Thus far we have studied the Raman effect in AlGaAs waveguides for 285 fs pulses. However, since the Raman terms in Eq. (3.9) are inversely proportional to the pulse width, the Raman effect becomes increasingly important for shorter pulses. Intuitively, a shorter pulse and its wider spectrum can excite a broader Raman gain. Figure 6 plots the energy exchange caused by the Raman effect as a function of pulse width under the π phase shift conditions. The dots are simulation results and the solid curve is an inverse function. The cross-talk between two orthogonally polarized pulses is more than 15% for a pulse width shorter than 600 fs. Also, the spectral distortion is more serious at shorter pulse widths.

V. SUMMARY

In summary, we have reported the depolarized Raman gain spectra for $Al_{0.24}Ga_{0.76}As$ at pump wavelengths of 0.515 and 1.55 μm. The depolarized Raman gain at 100 cm^{-1} is about 10^{-10} cm/W/cm^{-1} at a 1.55 μm pump wavelength. Our pulse propagation model, which is consistent with the previous experimental data,[1] shows that the low frequency Raman gain in AlGaAs waveguides produces cross-talk between two orthogonally polarized pulses and spectral distortions. The cross-talk is inversely proportional to the pulse width. For 300-fs pulses, the cross-talk is about 30%. Since the Raman effect and the nonlinear refractive index are both $\chi^{(3)}$ related, they obey the same scaling laws for intensity and waveguide length dependence. Because the Raman effect scales inversely with pulse width, the Raman effect limits the minimum pulse width with which AlGaAs waveguides may be used for nonlinear refractive index applications.

ACKNOWLEDGMENTS

[1] M. N. Islam, C. E. Soccolich, R. E. Slusher, A. F. J. Levi, W. S. Hobson, and M. G. Young, J. Appl. Phys. **71**, 1927 (1992).
[2] S. T. Ho, C. E. Soccolich, M. N. Islam, W. S. Hobson, A. F. J. Levi, and R. E. Slusher, Appl. Phys. Lett. **59**, 2558 (1991).
[3] C. C. Yang, A. Villeneuve, G. I. Stegeman, C.-H. Lin, and H.-H. Lin, IEEE J. Quantum Electron. **QE-29**, 2934 (1993).
[4] K. Al-hemyari, C. N. Ironside, and J. S. Aitchison, IEEE J. Quantum Electron. **QE-28**, 10 (1992).
[5] A. Villeneuve, C. C. Yang, P. G. J. Wigley, G. I. Stegeman, J. S. Aitchison, and C. N. Ironside, Appl. Phys. Lett. **61**, 147 (1992).
[6] C. C. Yang, A. Villeneuve, G. I. Stegeman, and J. S. Aitchison, Opt. Lett. **17**, 710 (1992).
[7] J. P. Gordon, Opt. Lett. **11**, 662 (1986).
[8] M. H. Grimsditch, D. Olego, and M. Cardona, Phys. Rev. B **20**, 1758 (1979).
[9] M. Cardona, M. H. Grimsditch, and D. Olego, in *Light Scattering in Solids*, edited by J. L. Birman, H. Z. Cummins, and K. K. Rebane (Plenum, New York, 1979).
[10] Saint-Cricq, R. Carles, J. B. Renucci, A. Zwick, and M. A. Renucci, Solid State Commun. **39**, 1137 (1981).
[11] M. Cardona, in *Light Scattering in Solids*, edited by M. Cardona (Springer, Berlin, 1975).
[12] R. H. Stolen and E. P. Ippen, Appl. Phys. Lett. **22**, 276 (1973).
[13] R. H. Stolen, Phys. Chem. Glasses **11**, 83 (1970); R. W. Hellwarth, J. Cherlow, and T.-T. Yang, Phys. Rev. B **11**, 964 (1975); D. M. Krol and J. G. Van Lierop, J. Non-Cryst. Solids **63**, 131 (1984).
[14] Y. R. Shen, *The Principle of Nonlinear Optics* (Wiley, New York, 1984).
[15] C. R. Menyuk, Opt. Lett. **16**, 566 (1991).
[16] C. R. Menyuk, IEEE J. Quantum Electron. **QE-23**, 174 (1987); **25**, 2674 (1989).
[17] M. D. Dvorak, W. A. Schroeder, D. R. Andersen, A. L. Smirl, and B. S. Wherrett, IEEE J. Quantum Electron. **QE-30**, 256 (1994).